

Multi-entity Video Transformers for Fine-Grained Video Representation Learning

Matthew Walmer^{1*}Keyur Muzumdar²¹University of Maryland, College ParkRose Kanjirathinkal²Taipeng Tian²²MetaKai Sheng Tai²Abhinav Shrivastava¹

Abstract

The area of temporally fine-grained video representation learning aims to generate frame-by-frame representations for temporally dense tasks. In this work, we advance the state-of-the-art for this area by re-examining the design of transformer architectures for video representation learning. A salient aspect of our self-supervised method is the improved integration of spatial information in the temporal pipeline by representing multiple entities per frame. Prior works use late fusion architectures that reduce frames to a single dimensional vector before any cross-frame information is shared, while our method represents each frame as a group of entities or tokens. Our **Multi-entity Video Transformer (MV-Former)** architecture achieves state-of-the-art results on multiple fine-grained video benchmarks. MV-Former leverages image features from self-supervised ViTs, and employs several strategies to maximize the utility of the extracted features while also avoiding the need to fine-tune the complex ViT backbone. This includes a Learnable Spatial Token Pooling strategy, which is used to identify and extract features for multiple salient regions per frame. Our experiments show that MV-Former not only outperforms previous self-supervised methods, but also surpasses some prior works that use additional supervision or training data. When combined with additional pre-training data from Kinetics-400, MV-Former achieves a further performance boost. The code for MV-Former is available at https://github.com/facebookresearch/video_rep_learning.

1. Introduction

Self-Supervised Learning (SSL) has been a rapidly growing area of research, showing potential both to scale to massive data and to learn in environments where annotations are limited or expensive to generate [1, 2, 6, 9, 10, 21, 22, 24, 28, 51]. Video Representation Learning is definitely

*Work performed during an internship with Meta.

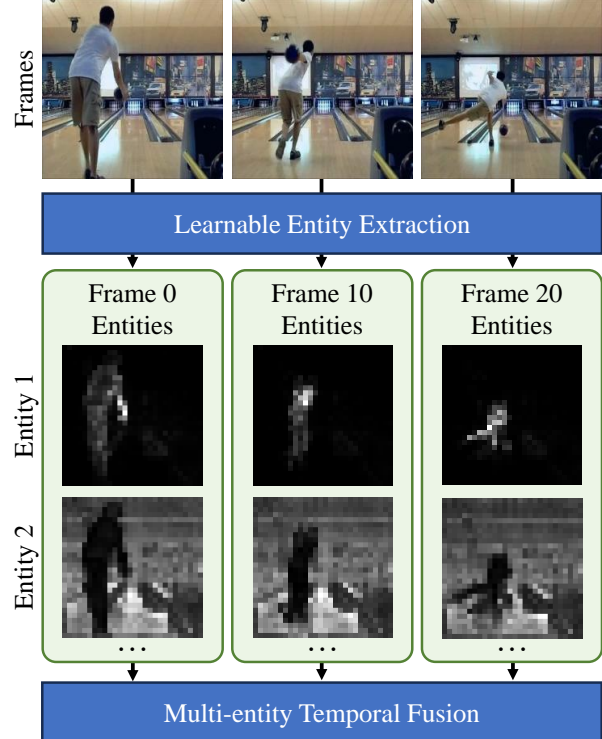


Figure 1. We present MV-Former, a Multi-entity Video Transformer architecture for fine-grained representation learning. MV-Former processes videos not as collections of frames but instead as collections of entities, and automatically learns to separate out the primary actor and scene background, as shown above for a sample video from the Penn Action dataset.

a good match for self-supervised learning [36, 37], though the majority of existing research in this space focuses on learning a single, video-level representation [11, 15, 16, 32, 35, 42, 44, 47, 49]. However, there are many tasks which require not only video-level understanding, but also a temporally dense understanding too. Such tasks include action phase classification [13, 27, 41, 53], fine-grained frame retrieval [13, 20], and video temporal alignment [4, 13, 19, 20]. The area of Fine-Grained Video Representation Learning

focuses on generating frame-wise features that are expressive and discriminative not only for high-level actions, but also the moment-to-moment steps that compose those actions [8, 13, 19, 20, 29, 38, 52]. Self-supervised learning is especially desirable for this domain, as frame-level video annotations are rare and expensive to create.

Networks for fine-grained video learning typically use a two-stage approach. First, a frame-level encoder is applied to reduce each frame into a single vector. Second, a temporal fusion module is applied, which allows information to flow between the representations of separate frames. Early works in this field utilized 3D convolutional networks to perform temporal fusion [7, 14, 43, 45], but recent works have shifted to transformer-based temporal fusion [8, 52]. Transformer fusion allows models to learn long-range inter-frame dynamics through self-attention. However, we believe past architectures are still quite limited in how they model information over the temporal axis. Prior approaches reduce each frame to a single 1D vector before any inter-frame information is shared. We believe this bottleneck limits the ability of models to represent multiple entities across frames, which restricts their capacity to learn the temporal dynamics of a scene. We present an architecture which aims to alleviate this bottleneck.

In this work, We re-examine the design of transformer-based architectures for self-supervised video representation learning, and propose a new **Multi-entity Video Transformer (MV-Former)** which achieves state-of-the-art performance on multiple fine-grained video benchmarks. Central to our approach for MV-Former is the choice to not parse videos as collections of frames, but instead as collections of salient entities, such as the primary actor and the scene background. We call this method **Multi-entity Temporal Fusion (MTF)**. Our approach is based on the intuition that videos contain multiple elements with distinct temporal dynamics. For example, the main human actor in an action recognition video may move rapidly, while the background moves very little. We extract multiple entities per frame with consistent semantics using a **Learnable Spatial Token Pooling (LSTP)** strategy. We show that LSTP is able to effectively identify the primary actor in the scene with absolutely no supervision. We transition away from the CNN-based backbones used in prior works [8, 38, 52], and opt for a fully-transformer-based architecture that leverages self-supervised ViTs for frame-level feature extraction. We also present several strategies to maximize the utility of these features, including the use of intermediate layer features. Overall, our MV-Former architecture advances the state-of-the-art for self-supervised models on the Penn Action [38] and FineGym [39] datasets. Furthermore, we demonstrate the improved strength of MV-Former when combined with large-scale pretraining on the Kinetics-400 dataset [7]. In summary, our contributions are as follows:

- **MV-Former**, a Multi-entity Video Transformer architecture for Self-Supervised Fine-Grained Video Representation Learning.
- State-of-the-art results for several benchmarks and metrics. MV-Former even surpasses some prior works that use additional supervision or training data.
- **Multi-entity Temporal Fusion**, which fuses information across the temporal axis by first parsing a scene into a collection of salient entities.
- Several strategies that help to maximize the utility of self-supervised ViT features while avoiding the need for backbone fine-tuning. This includes **Learnable Spatial Token Pooling** and multi-layer features.

2. Related Work

2.1. Self-Supervised Vision Transformers

Significant advances have been made in recent years in learning self-supervised visual representations, with many works focused on the recently popularized Vision Transformer (ViT) architecture [12]. As of writing, the most popular methods are contrastive or joint-embedding-based methods [6, 9, 18, 22, 31], and masked-reconstruction methods [3, 21]. Many works also focus on interpreting and comparing the properties of ViT features learned by these methods [17, 25, 40, 46]. In this work, we leverage DINO [6] features for use in a fine-grained video representation learning framework. Furthermore, we present extraction strategies to maximize their utility for such tasks while avoiding the need for backbone fine-tuning.

2.2. Self-Supervised Learning for Video

Many works have been proposed that translate advances in image-level SSL to the video domain. [15] demonstrated a unified framework to extend methods like MoCo [22], BYOL [18], SimCLR [9], and SwAV [5] into video-level methods by learning to maximize the similarity of representations of different clips from the same video. Several works focus on applying masked-reconstruction-based methods to video SSL through methods like temporal masking and reconstruction [16, 42, 44, 48, 49]. Other works focus on learning temporally stable representations by combining wide and narrow views of time [11, 14, 26, 33–35, 47, 50]. Note that these methods usually focus on learning video-level representations that are invariant to changes along the temporal axis. While such representations are beneficial for high-level video understanding, they are not helpful for tasks that require fine-grained, frame-level understanding.

2.3. Fine-Grained Video Representation Learning

The goal of Fine-Grained Video Representation Learning is to generate dense, frame-level features for tasks

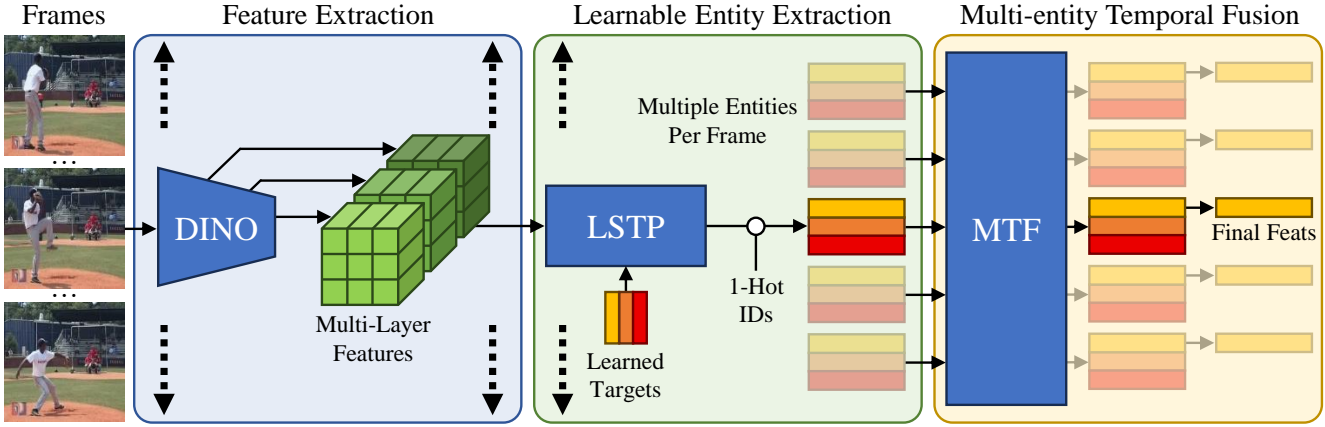


Figure 2. Summary of our MV-Former Architecture, which can be broken into three major phases: Feature Extraction, Learnable Entity Extraction, and Multi-entity Temporal Fusion (MTF). Multi-layer features are extracted from a DINO ViT backbone, and fed into our proposed Learnable Spatial Token Pooling layer (LSTP) which uses learned embedding targets to select which information to extract. This generates multiple entity features per frame, which are passed to the Multi-entity Temporal Fusion module. For final per-frame feature outputs, we use either a “CLS-style” approach (shown above), or an average-pooling of the separate entity outputs.

such as video alignment [4, 13, 19, 20], per-frame action classification [13, 27, 41, 53], and fine-grained frame retrieval [13, 20]. Much of the research in this field focuses on either self-supervised or weakly-supervised learning methods to reduce or remove the need for costly temporally dense annotations. [38] proposed Time-Contrastive Networks (TCN) and established the Pouring dataset. [13] proposed Temporal Cycle-Consistency (TCC) learning and also created additional annotations and benchmarking procedures for the Pouring and Penn Action [53] datasets. [8] greatly advanced self-supervised performance by proposing Sequence Contrastive Loss (SCL) and also by applying transformer-based temporal fusion. [52] further proposes a statistically-motivated learning objective using Brownian Bridges. Note that [8] and [52] use the same video learning architecture, which is comprised of a frame-level ResNet [23] followed by a video-level temporal fusion transformer. In this work, we re-visit the design of the overall video learning architecture, and present a new fully transformer-based architecture, MV-Former.

3. MV-Former Architecture

3.1. Design Motivation

We now describe our proposed **Multi-entity Video Transformer** architecture. MV-Former is designed to parse video scenes not as individual frames, but instead as collections of entities. In this work, we use the term “entity” to describe any region of the image with a shared semantic meaning. Under this definition, an entity can describe a person, an object, or even the entire background of the scene. Though the background may be composed of many separate objects (floors, walls, furniture, *etc.*) for purposes of parsing

the video it can all be grouped together as a single entity.

In our MV-Former architecture, we extract multiple entities per frame and associate them across time through a shared ID-vector. Our motivation for this approach is based on the intuition that video scenes contain multiple entities with distinct temporal dynamics. For example, in a video of a human performing an action, the person’s pose is often highly dynamic, changing rapidly from frame to frame. Meanwhile, the scene background is largely static, changing little throughout the video, especially in the case of short clips. The design of MV-Former can be separated into three major components: the per-frame Visual Backbone, the Learnable Spatial Token Pooling module, and the Multi-entity Temporal Fusion module. We will next describe each of these components.

3.2. Backbone and Features

Prior works in fine-grained video representation learning have typically relied on a ResNet-50 [23] backbone for extracting per-frame visual features. While ResNet-50 is popular both for its efficiency and effective features, more recent advances in Vision Transformers (ViTs) [12] and image-level self-supervised learning methods [6, 21, 22, 31] have produced more robust self-supervised features. In this work, we use features produced by DINO (v1) ViT models [6]. Specifically, we work with DINO-B/8, as its larger size and smaller patch resolution provide finer detail for local object features. These models produce powerful representations both at a global level and at a local level in the form of spatial token features. Prior works have demonstrated that these local features align well with object boundaries and semantics [6], so they are well-suited for extracting features for multiple entities per frame. It has also been shown

that the alignment of DINO feature semantics with local objects and object parts varies depending on their depth in the network [46]. For this reason, we use a multi-layer feature extraction strategy and take spatial token features from multiple intermediate layers. Unlike [8], we do not need to fine-tune the frame-level backbone, which is highly beneficial for training efficiency.

3.3. Learnable Spatial Token Pooling

After the frame-level backbone, MV-Former must identify and extract multiple entities from the spatial token features. Cross attention is a desirable mechanism for this purpose, as it can flexibly and dynamically extract features from regions of different shapes and sizes. We draw inspiration from [30] which uses the text-encoder of a CLIP model to guide self-supervised segmentation through cross attention on the visual token features. As we are working with DINO, a vision-only model, there are no language encoder features to guide this cross attention. Instead we propose a **Learnable Spatial Token Pooling (LSTP)**, which uses learnable embedding vectors for the cross attention input. These embedding vectors are trained as parameters along with the rest of the network, and they allow the network to learn which features are worth extracting from the scene. The number of learnable embedding vectors determines the number of entities extracted per frame. In our primary results, we use 3 or 6 entities per frame depending on the dataset. We also present an ablation in Section 5.4 with several different entity counts. These learnable embedding targets are held constant along the temporal dimension and across all samples at inference time. In this way, the Learnable Spatial Token Pooling module learns to extract consistent features for the most salient objects and image regions.

3.4. Multi-Entity Temporal Fusion

Finally, we fuse the per-frame per-entity features across the temporal dimension using a **Multi-entity Temporal Fusion (MTF)** module. The purpose of this module is to generating dense, per-frame features that are enriched through temporal context. Like [8], we use a three block transformer to perform fusion of the frame-level features. However, rather than feed in a single token per frame, we input multiple tokens per frame to represent the multiple entities extracted through Learnable Spatial Token Pooling. To differentiate the entities, we append a one-hot ID vector to the end of each entity feature vector during token generation. Due to this multi-entity approach, the effective “width” of the transformer is multiplied by the number of entities, however this does not increase the number of parameters. To provide a uniform baseline of comparison, we also present a “fixed-width” baseline in Section 5.4 which simulates the increased width of our MTF module.

For a standard transformer architecture, the number of

input tokens will be equal to the number of output tokens, meaning a separate feature is generated per input entity. To reduce this to a single output feature per frame, we consider two options. The first is to simply take the average of all the separate tokens. The second is an approach similar to how CLS tokens are used in classification ViTs, by designating the first token of each frame to act as the output token. This provides greater flexibility than average pooling, which tends to provide similar gradients to each of the separate entity tokens. We find that the averaging approach performs better for Classification and Retrieval, while the CLS-style approach works better for Phase Progression.

4. Experimental Methods

4.1. Datasets

We follow the protocols of [13] and [8] and conduct benchmarking experiments on three video datasets: Penn Action [53], FineGym [39], and Pouring [38]. For FineGym, we conduct experiments on two different splits, FineGym99 and FineGym288. FineGym288 has additional category labels and additional training data. All of our experiments are trained self-supervised without labels, so for FineGym288 we utilize the extra training data but not the extra label information. Additionally, we conduct experiments with large-scale pretraining on Kinetics-400 [7].

4.2. Tasks and Metrics

We compare against prior works using four standard tasks and metrics. **(1) Phase Classification:** In this task, videos have been annotated on a frame-by-frame level by dividing the actions into key phases. After self-supervised training, the model is frozen and a linear classifier is trained to predict the action phases. Classification accuracy is reported. **(2) Phase Progression:** For each frame, the model must predict how much time is left until the next action phase boundary. A linear regression model is trained on top of the frozen network, and the average R-squared metric is reported. **(3) Kendall’s Tau:** Given two frames from two different videos, the model must match the frames such that the pairs have the same temporal ordering. This is achieved through nearest neighbors matching. Fraction of correct matches is reported. **(4) Fine-Grained Frame Retrieval:** Given a query frame, the goal is to return k frames with the same fine-grained frame action label as the query. We report results for Average Precision with $k = 5$ (AP@5). For additional details on the tasks and metrics, please see [8, 13].

4.3. Baselines

In this work, we focus on comparing with other works that learn video representation in a fully self-supervised way. This includes SaL [29], TCN [38], CARL [8], and VSP [52]. Over the years, many methods have been pro-

Table 1. Self-supervised results on Penn Action and FineGym. We achieve state-of-the-art self-supervised results on all four metrics for Penn Action, and our results are at least 2 standard deviations ahead of the prior bests. For FineGym we also achieve state-of-the-art performance for Phase Classification on both splits tested.

Method	Penn Action				FineGym	
	Classification	Progress	Tau	Retrieval	Classification (99)	Classification (288)
SaL [29]	68.15	0.390	0.474	76.04	21.45	19.58
TCN [38]	68.09	0.383	0.542	77.84	20.02	17.11
CARL [8]	93.07	0.918	0.985	92.28	41.75	35.23
VSP [52]	93.12	0.923	0.986	92.56	43.12	36.95
MV-F (ours)	94.21 \pm 0.04	0.931 \pm 0.006	0.989 \pm 0.002	92.99 \pm 0.06	44.77 \pm 0.71	38.30 \pm 0.26

posed that use different levels of weakly supervised data, included paired video samples [13, 20], or phase boundary time stamps [52]. We present a comprehensive comparison with weakly and fully supervised methods in the supplemental material.

4.4. Training Details

For our frame-level backbone, we utilize DINO ViT-B/8 [6]. We find that some datasets benefit from features derived from earlier layers, while others prefer features derived from only later layers. We extract features from layers 4, 8, and 12 when working with Penn Action and Kinetics-400, and from layers 9, 10, and 11 when working with FineGym. For Pouring, we use only the final layer features, as using extra features is detrimental due to the very small size of the dataset. For Penn Action, Pouring, and Kinetics-400, we use 3 entities per frame, and for FineGym we increase this to 6 entities per frame. We use a CLS-style final feature selection strategy for Penn Action, Pouring, and Kinetics-400, and we use the average-pooling strategy for FineGym. We train MV-Former using Sequence Contrastive Loss (SCL) [8]. For Pouring, Penn Action, FineGym99/288, and Kinetics-400, we train for 1000, 500, 300, and 10 epochs respectively. On Penn Action and Pouring, we train with a batch size of 4 on 4 A100 GPUs, and for FineGym and Kinetics-400 pretraining we use a batch size of 8 on 8 A100 GPUs.

4.5. Measuring the Impact of Initialization

For our evaluation protocols, we make one major change from prior works, as we choose to measure and report results for multiple random initialization per model configuration and dataset. For any optimization procedure, the final state of the network will depend on the initial state, but a well-performing network and objective together should converge to a good solution consistently, regardless of the initial state. We believe it is important to consider the impact of the random network initialization on the quality of the final network. While prior works report results for only

Table 2. Self-supervised results on the Pouring dataset. Due to the small dataset size and the increased complexity of MV-Former, we do not see improved results for most metrics. For Retrieval, MV-Former’s average performance surpasses the baselines, however the small size of Pouring also causes much higher variance in the metrics. For CARL*, we re-run the CARL baseline for three random trials, and again observe high variance.

Method	Pouring			
	Class.	Progress	Tau	Retrieval
SaL	-	-	-	84.05
TCN	89.53	0.804	0.852	83.56
CARL	93.73	0.935	0.992	-
VSP	93.85	0.942	0.990	91.85
CARL*	89.95 ± 3.33	0.873 ± 0.047	0.970 ± 0.007	89.21 ± 0.80
MV-F	93.34 ± 2.00	0.919 ± 0.015	0.985 ± 0.003	92.33 \pm 1.02

one trial per model, we instead adopt a multi-trial protocol. Specifically, in each test we conduct three trials with different random initialization seeds, and we report all results as the mean plus/minus two standard deviations.

Through this protocol, we show that MV-Former achieves state-of-the-art performance on Penn Action and FineGym by a statistically significant margin. This also allows us to measure the variance of the four commonly used benchmark tasks and metrics. We identify that the Phase Progression task and metric has the highest sensitivity to the model initialization. We encourage future works in this area to adopt a similar multi-trial methodology.

5. Results

5.1. Primary Results

Penn Action. As shown in Table 1, MV-Former achieves state-of-the-art self-supervised performance in all four metrics for Penn Action. The largest gain is achieved in Classification, with an increase of 1.09% over VSP. For all four metrics, our improvement is at least two standard deviations above the best performing prior work. We note that the Phase Progression metric has the highest standard de-

Table 3. Self-supervised results with Kinetics-400 pretraining. MV-Former achieves state-of-the-art performance in Classification and Retrieval, however performance is degraded in Progress and Tau. This matches the trend for CARL, which is also trained with SCL. The highest score for each metric is **bold** and the second highest is underlined.

Method	Pre.	Fine.	Kinetics-400 → Penn Action			
			Classification	Progress	Tau	Retrieval
CARL	w/o Pre.		93.07	0.918	0.985	92.28
CARL	✓		91.9	0.903	0.949	-
CARL	✓	✓	93.9	0.908	0.977	-
VSP	w/o Pre.		93.12	0.923	0.986	92.56
VSP	✓		92.35	0.894	0.952	-
VSP	✓	✓	93.57	0.944	<u>0.988</u>	-
MV-F	w/o Pre.		<u>94.21 ± 0.04</u>	<u>0.931 ± 0.006</u>	0.989 ± 0.002	<u>92.99 ± 0.06</u>
MV-F	✓		91.62 ± 0.30	0.927 ± 0.005	0.895 ± 0.004	88.38 ± 0.20
MV-F	✓	✓	94.56 ± 0.32	0.924 ± 0.004	0.980 ± 0.002	93.40 ± 0.08

viation relative to its absolute value, showing that it is the most sensitive to the random network initialization. Meanwhile, Classification and Retrieval both have relatively low sensitivity to initialization.

FineGym. We report fine-grained classification accuracy on both splits FineGym99 and FineGym288 in Table 1. Once again, MV-Former achieve state-of-the-art self-supervised results for Phase Classification on both splits. MV-Former’s average score surpasses VSP by 1.65% for FineGym99 and 1.35% for FineGym288.

Pouring. We present results on the Pouring dataset in Table 2. Unfortunately, MV-Former does not surpass the prior works in Classification, Progress, or Tau, though it does advance performance in Retrieval. We believe this is due to the increased complexity of MV-Former and the very small size of the Pouring dataset. The training set for Pouring contains only 70 videos, making it roughly 16 times smaller than Penn Action and 45 times smaller than FineGym99. We also note that the metrics have much higher variance on Pouring, also likely due to the small dataset size. To further illustrate this issue, we present results re-running the CARL baseline method for three random trials, denoted as “CARL*” in Table 2, and we find that it also shows high variance for the Pouring metrics.

5.2. Large Scale Pretraining

We show that MV-Former can achieved further performance improvements on the Penn Action dataset through large-scale pre-training on Kinetics-400. We again follow our 3-trial experimental protocol and pre-train three different MV-Formers on Kinetics-400 for 10 epochs, and then finetune them on Penn Action for 500 epochs. The results are summarized in Table 3. We see that Kinetics-400 pretraining boosts Classification performance by another 0.35%, putting it almost 1% ahead of the similar VSP model with Kinetics-400 pretraining and finetuning. We also see

a 0.41% gain in Retrieval. However, we find that pretraining is actually detrimental for the Progress and Tau metrics. This trend matches the numbers reported for CARL, which is also trained using SCL.

5.3. Visualizing Learnable Spatial Token Pooling

To better illustrate the function of our Multi-entity Temporal Fusion strategy, we visualize the attention maps created by the Learnable Spatial Token Pooling (LSTP) module. LSTP is responsible for selecting the features for each entity by learning which image regions to attend to through cross-attention. We take several sample videos from the Penn Action dataset and visualize the LSTP attention maps for our best performing MV-Former model in Figure 3. For the first entity, LSTP has learned to attend to the primary actor in each scene, with a particular focus on the person’s limbs. Under our CLS-style output configuration, the first entity is the token that is taken as the final output, so it makes sense it would focus on the most important part of the scene. Meanwhile, the second entity consistently cuts out the image background, including removing other people in the scene, like the umpire shown in the first sample. Note that the regions of attention do not have to be distinct or disjoint. In this case, the third entity (not shown) also attends to the primary actor in the scene. This is reasonable, as the person is certainly the most important thing to attend to in a human action dataset/task. These visualization demonstrate that LSTP automatically learns to segment out the primary actor and background in human action videos without any explicit supervision.

5.4. Ablations

Finally, we present several ablations of MV-Former design elements, summarized in Table 4.

ResNet Backbone. To begin, in row 1 we compare with the same architecture used by [8] and [52], which uses a



Figure 3. Visualization of the attention maps for the Learnable Spatial Token Pooling layers across multiple frames and sample videos. We see that for the first entity, which is also the output token, the focus is set on the primary actor in the scene, with particular focus on the position of their limbs. The second entity meanwhile focuses on the scene background.

ResNet-50 backbone, per-frame feature max-pooling, and one token per frame. For these trials, we keep the ResNet backbone frozen and do not perform partial backbone fine-tuning like [8]. As a result, the scores are slightly lower than those reported by [8], except for Kendall’s Tau, which will be discussed later. We then apply LSTP and MTF to the ResNet backbone, to demonstrate their effectiveness with non-DINO features. We test with 1, 3, and 5 entities in rows 2 – 4. We find that using LSTP with only one entity is very beneficial for Classification and Retrieval, and slightly beneficial for Progress. Increasing the number of entities to 3 or 5 is better for Progress but less beneficial for Classification and Retrieval. This suggests that these two groups of metrics may sometimes be contradictory in terms of what model design is best. Kendall’s Tau is fairly stable for all four configurations.

Backbone and Feature Pooling. Next, in rows 5-7 we replace the backbone with DINO ViT-B/8 and apply three different strategies for per-frame feature selection: max pooling of spatial token features, average pooling, and CLS token features. Max pooling aligns most closely with the original architecture of [8], however, for a ViT backbone it yields poor results in three of the four metrics. Average pooling is also a standard choice, and it does give much

better performance in all metrics except Tau. For a ViT, it is also natural to take the CLS token as a built-in global representation. Indeed, using the CLS token is the best of these three options, and it gives a good performance boost in Classification, Progress, and Retrieval.

LSTP, MTF, and Entity Count. We follow this by adding Learnable Spatial Token Pooling and Multi-entity Temporal Fusion with 1, 3, or 5 entities per frame (rows 8–10). Note that applying LSTP with only one learnable entity (row 8) is equivalent to ablating MTF. It is also functionally very similarly to using the CLS token features, though with the disadvantage of needing to retrain the attention layers from scratch. As a result, LSTP with 1 entity does worse than CLS in Classification and Retrieval, though slightly better in Phase Progression. The strength of LSTP truly comes when used in combination with MTF. As seen in row 9, using LSTP with MTF with 3 entities increases all metrics except Kendall’s Tau. However, increasing the number of entities too high can be detrimental, as shown by the 5 entity version in row 10.

Fixed Width Baseline. As an extra comparison, we present a “fixed-width” baseline to show that the performance benefits of MTF are not simply a consequence of its increased width. To do this, we create a model that sim-

Table 4. Ablation of MV-Former design contributions on the Penn Action dataset, including the DINO backbone, Learnable Spatial Token Pooling, Multi-entity Temporal Fusion, and multi-layer feature extraction. The model in row 14 is our final MV-Former version presented for Penn Action in the primary results above. In rows 11 and 12 we simulate the increased width of MTF without the benefits of modeling multiple entities by generating multiple tokens from the backbone CLS token. The highest score for each metric is **bold** and the second highest is underlined.

	Backbone	Feat. Layer(s)	Feat. Pool	Ent.	MTF	Classification	Progress	Tau	Retrieval
1	ResNet-50	Last	Max	-	no	91.96 ± 0.48	0.900 ± 0.008	0.993 ± 0.001	90.88 ± 0.38
2	ResNet-50	Last	LSTP	1	no	92.77 ± 0.08	0.909 ± 0.008	0.991 ± 0.001	91.50 ± 0.23
3	ResNet-50	Last	LSTP	3	yes	92.46 ± 0.24	0.915 ± 0.002	0.992 ± 0.0004	91.15 ± 0.20
4	ResNet-50	Last	LSTP	5	yes	92.54 ± 0.25	0.917 ± 0.004	0.992 ± 0.001	91.28 ± 0.20
5	DINO-B/8	Last	Max	-	no	87.61 ± 0.12	0.883 ± 0.005	0.996 ± 0.0001	83.76 ± 0.21
6	DINO-B/8	Last	Avg	-	no	92.57 ± 0.07	0.904 ± 0.012	<u>0.995 ± 0.001</u>	90.52 ± 0.4
7	DINO-B/8	Last	CLS	-	no	93.48 ± 0.16	0.918 ± 0.007	0.992 ± 0.0002	92.31 ± 0.16
8	DINO-B/8	Last	LSTP	1	no	93.35 ± 0.61	0.924 ± 0.006	0.990 ± 0.0001	91.97 ± 0.79
9	DINO-B/8	Last	LSTP	3	yes	93.92 ± 0.24	<u>0.926 ± 0.004</u>	0.989 ± 0.0003	92.81 ± 0.30
10	DINO-B/8	Last	LSTP	5	yes	93.50 ± 0.27	0.911 ± 0.006	0.992 ± 0.001	92.50 ± 0.3
11	DINO B/8	Last	CLS+FC	3*	no	88.28 ± 0.48	0.913 ± 0.008	0.995 ± 0.0002	86.49 ± 0.27
12	DINO B/8	Last	CLS+FC	5*	no	87.97 ± 0.12	0.911 ± 0.004	0.995 ± 0.0001	86.26 ± 0.12
13	DINO-B/8	4,8,12	LSTP	1	no	94.23 ± 0.08	0.920 ± 0.007	0.987 ± 0.0005	<u>93.02 ± 0.18</u>
14	DINO-B/8	4,8,12	LSTP	3	yes	<u>94.21 ± 0.04</u>	0.931 ± 0.006	0.989 ± 0.002	92.99 ± 0.06
15	DINO-B/8	4,8,12	LSTP	5	yes	94.11 ± 0.18	<u>0.926 ± 0.005</u>	0.989 ± 0.002	93.07 ± 0.01

ulates the extra width of MTF without using LSTP, by instead generating multiple tokens per frame directly from the backbone CLS token representation. This is achieved using an extra fully-connected layer to split the CLS token features into 3 or 5 separate feature vectors. From the results in rows 11 and 12, we can see that simply increasing the width of the fusion module is not beneficial, and that separating out the CLS token may actually be detrimental. This also demonstrates that the LSTP mechanism is able to extract multiple useful token representations from each frame.

Multi-Layer Feature Extraction. Finally, in rows 13 – 15 we measure the performance with multi-layer feature extraction. We find that the extra features are generally beneficial for most metrics. Minor differences in the model settings may slightly favor some metrics over others. However, we find that using 3 entities with multi-layer features is the best all-around performer. This model, as shown in row 14, is our final MV-Former model presented above.

Kendall’s Tau and Model Complexity. In Table 4, for Classification, Progress, and Retrieval, we see a general trend where more complex models tend to achieve better performance. However, for Kendall’s Tau this trend is reversed, favoring simpler feature extraction and fusion strategies. This further illustrates the potentially contradictory nature of these four commonly used metrics. Overall, the scores for Tau are quite close to 1.0, so we believe minor variations in the Kendall’s Tau score are not majorly representative of model quality.

6. Conclusion

In this work, we have presented MV-Former, a Multi-entity Video Transformer which parses scenes into multiple entities before performing transformer-based temporal fusion. We refer to this approach as Multi-entity Temporal Fusion, which is distinct from prior works where each frame must be reduced to a single vector representation before any information is shared between frames. To generate these entities, we also propose a cross-attention-based Learnable Spatial Token Pooling strategy, which uses trainable query embeddings to learn which information to extract from each frame. We show through visualizations that this approach naturally learns to separate out the primary actor in each scene and the background. MV-Former is a fully transformer-based framework for fine-grained video representation learning, which achieves state-of-the-art results on the Penn Action and FineGym datasets. We also show how MV-Former benefits from large-scale pretraining on Kinetics-400, further advancing performance in classification and retrieval, surpassing some prior methods which use weak or full supervision.

Limitations & Future Work. We have seen that MV-Former is effective at learning to separate out the primary actor in the scene as well as the background. However, it is not effective at identifying and segmenting other important objects, like the weights in a weight lifting scene for example. We believe this occurs because the learned queries used by LSTP are shared for all inference samples, and thus

they learn to focus on the concepts that are most universal across the dataset categories. In the future, we would like to examine potential ways to improve LSTP’s ability to identify category-dependent salient objects, possibly by applying language-based weak supervision. In addition, while we have demonstrated the effectiveness of MV-Former when trained with SCL, we would also like to test it with additional self-supervised and weakly-supervised methods, such as TCC, TCN, and VSP.

Acknowledgements. We would like to thank our peers Chao-Yuan Wu, Sumedha Singla, and Florian Metze for their valuable feedback and suggestions for this work.

References

- [1] Philip Bachman, R Devon Hjelm, and William Buchwalter. Learning representations by maximizing mutual information across views. *Advances in neural information processing systems*, 32, 2019. [1](#)
- [2] Randall Balestrieri, Mark Ibrahim, Vlad Sobal, Ari Mornos, Shashank Shekhar, Tom Goldstein, Florian Bordes, Adrien Bardes, Gregoire Mialon, Yuandong Tian, et al. A cookbook of self-supervised learning. *arXiv preprint arXiv:2304.12210*, 2023. [1](#)
- [3] Hangbo Bao, Li Dong, Songhao Piao, and Furu Wei. Beit: Bert pre-training of image transformers. *arXiv preprint arXiv:2106.08254*, 2021. [2](#)
- [4] Kaidi Cao, Jingwei Ji, Zhangjie Cao, Chien-Yi Chang, and Juan Carlos Niebles. Few-shot video classification via temporal alignment. In *Proceedings of the IEEE/CVF Conference on Computer Vision and Pattern Recognition*, pages 10618–10627, 2020. [1, 3](#)
- [5] Mathilde Caron, Ishan Misra, Julien Mairal, Priya Goyal, Piotr Bojanowski, and Armand Joulin. Unsupervised learning of visual features by contrasting cluster assignments. *Advances in neural information processing systems*, 33:9912–9924, 2020. [2](#)
- [6] Mathilde Caron, Hugo Touvron, Ishan Misra, Hervé Jégou, Julien Mairal, Piotr Bojanowski, and Armand Joulin. Emerging properties in self-supervised vision transformers. In *Proceedings of the IEEE/CVF international conference on computer vision*, pages 9650–9660, 2021. [1, 2, 3, 5](#)
- [7] Joao Carreira and Andrew Zisserman. Quo vadis, action recognition? a new model and the kinetics dataset. In *proceedings of the IEEE Conference on Computer Vision and Pattern Recognition*, pages 6299–6308, 2017. [2, 4](#)
- [8] Minghao Chen, Fangyun Wei, Chong Li, and Deng Cai. Frame-wise action representations for long videos via sequence contrastive learning. In *Proceedings of the IEEE/CVF Conference on Computer Vision and Pattern Recognition*, pages 13801–13810, 2022. [2, 3, 4, 5, 6, 7, 12](#)
- [9] Ting Chen, Simon Kornblith, Mohammad Norouzi, and Geoffrey Hinton. A simple framework for contrastive learning of visual representations. In *International conference on machine learning*, pages 1597–1607. PMLR, 2020. [1, 2](#)
- [10] Xinlei Chen, Haoqi Fan, Ross Girshick, and Kaiming He. Improved baselines with momentum contrastive learning. *arXiv preprint arXiv:2003.04297*, 2020. [1](#)
- [11] Ishan Dave, Rohit Gupta, Mamshad Nayeem Rizve, and Mubarak Shah. Tclr: Temporal contrastive learning for video representation. *Computer Vision and Image Understanding*, 219:103406, 2022. [1, 2](#)
- [12] Alexey Dosovitskiy, Lucas Beyer, Alexander Kolesnikov, Dirk Weissenborn, Xiaohua Zhai, Thomas Unterthiner, Mostafa Dehghani, Matthias Minderer, Georg Heigold, Sylvain Gelly, et al. An image is worth 16x16 words: Transformers for image recognition at scale. *arXiv preprint arXiv:2010.11929*, 2020. [2, 3](#)
- [13] Debidatta Dwibedi, Yusuf Aytar, Jonathan Tompson, Pierre Sermanet, and Andrew Zisserman. Temporal cycle-consistency learning. In *Proceedings of the IEEE/CVF conference on computer vision and pattern recognition*, pages 1801–1810, 2019. [1, 2, 3, 4, 5, 12](#)
- [14] Christoph Feichtenhofer, Haoqi Fan, Jitendra Malik, and Kaiming He. Slowfast networks for video recognition. In *Proceedings of the IEEE/CVF international conference on computer vision*, pages 6202–6211, 2019. [2](#)
- [15] Christoph Feichtenhofer, Haoqi Fan, Bo Xiong, Ross Girshick, and Kaiming He. A large-scale study on unsupervised spatiotemporal representation learning. In *Proceedings of the IEEE/CVF Conference on Computer Vision and Pattern Recognition*, pages 3299–3309, 2021. [1, 2](#)
- [16] Christoph Feichtenhofer, Yanghao Li, Kaiming He, et al. Masked autoencoders as spatiotemporal learners. *Advances in neural information processing systems*, 35:35946–35958, 2022. [1, 2](#)
- [17] Quentin Garrido, Yubei Chen, Adrien Bardes, Laurent Najman, and Yann Lecun. On the duality between contrastive and non-contrastive self-supervised learning. *arXiv preprint arXiv:2206.02574*, 2022. [2](#)
- [18] Jean-Bastien Grill, Florian Strub, Florent Altché, Corentin Tallec, Pierre Richemond, Elena Buchatskaya, Carl Doersch, Bernardo Avila Pires, Zhaohan Guo, Mohammad Gheshlaghi Azar, et al. Bootstrap your own latent-a new approach to self-supervised learning. *Advances in neural information processing systems*, 33:21271–21284, 2020. [2](#)
- [19] Isma Hadji, Konstantinos G Derpanis, and Allan D Jepson. Representation learning via global temporal alignment and cycle-consistency. In *Proceedings of the IEEE/CVF Conference on Computer Vision and Pattern Recognition*, pages 11068–11077, 2021. [1, 2, 3, 12](#)
- [20] Sanjay Haresh, Sateesh Kumar, Huseyin Coskun, Shahram N Syed, Andrey Konin, Zeeshan Zia, and Quoc-Huy Tran. Learning by aligning videos in time. In *Proceedings of the IEEE/CVF Conference on Computer Vision and Pattern Recognition*, pages 5548–5558, 2021. [1, 2, 3, 5, 12](#)
- [21] Kaiming He, Xinlei Chen, Saining Xie, Yanghao Li, Piotr Dollár, and Ross Girshick. Masked autoencoders are scalable vision learners. In *Proceedings of the IEEE/CVF Conference on Computer Vision and Pattern Recognition*, pages 16000–16009, 2022. [1, 2, 3](#)
- [22] Kaiming He, Haoqi Fan, Yuxin Wu, Saining Xie, and Ross Girshick. Momentum contrast for unsupervised visual rep-

resentation learning. In *Proceedings of the IEEE/CVF conference on computer vision and pattern recognition*, pages 9729–9738, 2020. 1, 2, 3

[23] Kaiming He, Xiangyu Zhang, Shaoqing Ren, and Jian Sun. Deep residual learning for image recognition. In *Proceedings of the IEEE conference on computer vision and pattern recognition*, pages 770–778, 2016. 3

[24] R Devon Hjelm, Alex Fedorov, Samuel Lavoie-Marchildon, Karan Grewal, Phil Bachman, Adam Trischler, and Yoshua Bengio. Learning deep representations by mutual information estimation and maximization. *arXiv preprint arXiv:1808.06670*, 2018. 1

[25] Klemen Kotar, Gabriel Ilharco, Ludwig Schmidt, Kiana Ehsani, and Roozbeh Mottaghi. Contrasting contrastive self-supervised representation learning pipelines. In *Proceedings of the IEEE/CVF International Conference on Computer Vision*, pages 9949–9959, 2021. 2

[26] Haofei Kuang, Yi Zhu, Zhi Zhang, Xinyu Li, Joseph Tighe, Sören Schwertfeger, Cyrill Stachniss, and Mu Li. Video contrastive learning with global context. In *Proceedings of the IEEE/CVF International Conference on Computer Vision*, pages 3195–3204, 2021. 2

[27] Hilde Kuehne, Ali Arslan, and Thomas Serre. The language of actions: Recovering the syntax and semantics of goal-directed human activities. In *Proceedings of the IEEE conference on computer vision and pattern recognition*, pages 780–787, 2014. 1, 3

[28] Ishan Misra and Laurens van der Maaten. Self-supervised learning of pretext-invariant representations. In *Proceedings of the IEEE/CVF conference on computer vision and pattern recognition*, pages 6707–6717, 2020. 1

[29] Ishan Misra, C Lawrence Zitnick, and Martial Hebert. Shuffle and learn: unsupervised learning using temporal order verification. In *Computer Vision–ECCV 2016: 14th European Conference, Amsterdam, The Netherlands, October 11–14, 2016, Proceedings, Part I 14*, pages 527–544. Springer, 2016. 2, 4, 5, 12

[30] Jishnu Mukhoti, Tsung-Yu Lin, Omid Poursaeed, Rui Wang, Ashish Shah, Philip HS Torr, and Ser-Nam Lim. Open vocabulary semantic segmentation with patch aligned contrastive learning. In *Proceedings of the IEEE/CVF Conference on Computer Vision and Pattern Recognition*, pages 19413–19423, 2023. 4

[31] Maxime Oquab, Timothée Darcet, Théo Moutakanni, Huy Vo, Marc Szafraniec, Vasil Khalidov, Pierre Fernandez, Daniel Haziza, Francisco Massa, Alaaeldin El-Nouby, et al. Dinov2: Learning robust visual features without supervision. *arXiv preprint arXiv:2304.07193*, 2023. 2, 3

[32] Rui Qian, Tianjian Meng, Boqing Gong, Ming-Hsuan Yang, Huiheng Wang, Serge Belongie, and Yin Cui. Spatiotemporal contrastive video representation learning. In *Proceedings of the IEEE/CVF Conference on Computer Vision and Pattern Recognition*, pages 6964–6974, 2021. 1

[33] Zhiwu Qing, Shiwei Zhang, Ziyuan Huang, Yi Xu, Xiang Wang, Mingqian Tang, Changxin Gao, Rong Jin, and Nong Sang. Learning from untrimmed videos: Self-supervised video representation learning with hierarchical consistency. In *Proceedings of the IEEE/CVF Conference on Computer Vision and Pattern Recognition*, pages 13821–13831, 2022. 2

[34] Kanchana Ranasinghe, Muzammal Naseer, Salman Khan, Fahad Shahbaz Khan, and Michael S Ryoo. Self-supervised video transformer. In *Proceedings of the IEEE/CVF Conference on Computer Vision and Pattern Recognition*, pages 2874–2884, 2022. 2

[35] Adria Recasens, Pauline Luc, Jean-Baptiste Alayrac, Luyu Wang, Florian Strub, Corentin Tallec, Mateusz Malinowski, Viorica Pătrăucean, Florent Altché, Michal Valko, et al. Broaden your views for self-supervised video learning. In *Proceedings of the IEEE/CVF International Conference on Computer Vision*, pages 1255–1265, 2021. 1, 2

[36] Madeline C Schiappa, Yogesh S Rawat, and Mubarak Shah. Self-supervised learning for videos: A survey. *ACM Computing Surveys*, 55(13s):1–37, 2023. 1

[37] Javier Selva, Anders S Johansen, Sergio Escalera, Kamal Nasrollahi, Thomas B Moeslund, and Albert Clapés. Video transformers: A survey. *IEEE Transactions on Pattern Analysis and Machine Intelligence*, 2023. 1

[38] Pierre Sermanet, Corey Lynch, Yevgen Chebotar, Jasmine Hsu, Eric Jang, Stefan Schaal, Sergey Levine, and Google Brain. Time-contrastive networks: Self-supervised learning from video. In *2018 IEEE international conference on robotics and automation (ICRA)*, pages 1134–1141. IEEE, 2018. 2, 3, 4, 5, 12

[39] Dian Shao, Yue Zhao, Bo Dai, and Dahua Lin. Finegym: A hierarchical video dataset for fine-grained action understanding. In *Proceedings of the IEEE/CVF conference on computer vision and pattern recognition*, pages 2616–2625, 2020. 2, 4

[40] Shashank Shekhar, Florian Bordes, Pascal Vincent, and Ari Morcos. Objectives matter: Understanding the impact of self-supervised objectives on vision transformer representations. *arXiv preprint arXiv:2304.13089*, 2023. 2

[41] Gunnar A Sigurdsson, Gülcin Varol, Xiaolong Wang, Ali Farhadi, Ivan Laptev, and Abhinav Gupta. Hollywood in homes: Crowdsourcing data collection for activity understanding. In *Computer Vision–ECCV 2016: 14th European Conference, Amsterdam, The Netherlands, October 11–14, 2016, Proceedings, Part I 14*, pages 510–526. Springer, 2016. 1, 3

[42] Hao Tan, Jie Lei, Thomas Wolf, and Mohit Bansal. Vimpac: Video pre-training via masked token prediction and contrastive learning. *arXiv preprint arXiv:2106.11250*, 2021. 1, 2

[43] Graham W Taylor, Rob Fergus, Yann LeCun, and Christoph Bregler. Convolutional learning of spatio-temporal features. In *Computer Vision–ECCV 2010: 11th European Conference on Computer Vision, Heraklion, Crete, Greece, September 5–11, 2010, Proceedings, Part VI 11*, pages 140–153. Springer, 2010. 2

[44] Zhan Tong, Yibing Song, Jue Wang, and Limin Wang. Videomae: Masked autoencoders are data-efficient learners for self-supervised video pre-training. *Advances in neural information processing systems*, 35:10078–10093, 2022. 1, 2

[45] Du Tran, Lubomir Bourdev, Rob Fergus, Lorenzo Torresani, and Manohar Paluri. Learning spatiotemporal features with 3d convolutional networks. In *Proceedings of the IEEE international conference on computer vision*, pages 4489–4497, 2015. 2

[46] Matthew Walmer, Saksham Suri, Kamal Gupta, and Abhinav Shrivastava. Teaching matters: Investigating the role of supervision in vision transformers. *arXiv preprint arXiv:2212.03862*, 2022. 2, 4

[47] Jue Wang, Gedas Bertasius, Du Tran, and Lorenzo Torresani. Long-short temporal contrastive learning of video transformers. In *Proceedings of the IEEE/CVF Conference on Computer Vision and Pattern Recognition*, pages 14010–14020, 2022. 1, 2

[48] Limin Wang, Bingkun Huang, Zhiyu Zhao, Zhan Tong, Yinan He, Yi Wang, Yali Wang, and Yu Qiao. Videomae v2: Scaling video masked autoencoders with dual masking. In *Proceedings of the IEEE/CVF Conference on Computer Vision and Pattern Recognition*, pages 14549–14560, 2023. 2

[49] Rui Wang, Dongdong Chen, Zuxuan Wu, Yinpeng Chen, Xiyang Dai, Mengchen Liu, Yu-Gang Jiang, Luwei Zhou, and Lu Yuan. Bevt: Bert pretraining of video transformers. In *Proceedings of the IEEE/CVF conference on computer vision and pattern recognition*, pages 14733–14743, 2022. 1, 2

[50] Fanyi Xiao, Kaustav Kundu, Joseph Tighe, and Davide Modolo. Hierarchical self-supervised representation learning for movie understanding. In *Proceedings of the IEEE/CVF Conference on Computer Vision and Pattern Recognition*, pages 9727–9736, 2022. 2

[51] Jure Zbontar, Li Jing, Ishan Misra, Yann LeCun, and Stéphane Deny. Barlow twins: Self-supervised learning via redundancy reduction. In *International Conference on Machine Learning*, pages 12310–12320. PMLR, 2021. 1

[52] Heng Zhang, Daqing Liu, Qi Zheng, and Bing Su. Modeling video as stochastic processes for fine-grained video representation learning. In *Proceedings of the IEEE/CVF Conference on Computer Vision and Pattern Recognition*, pages 2225–2234, 2023. 2, 3, 4, 5, 6, 12

[53] Weiyu Zhang, Menglong Zhu, and Konstantinos G Derpanis. From actemes to action: A strongly-supervised representation for detailed action understanding. In *Proceedings of the IEEE international conference on computer vision*, pages 2248–2255, 2013. 1, 3, 4

A. Comparison with Methods that use Additional Supervision

In Table 5 we present a comprehensive comparison of recent approaches on the Penn Action and FineGym dataset for fine-grained video representation tasks. In addition to self-supervised methods, we also compare with methods using weak or full supervision, and for Penn Action we also include methods using Kinetics-400 pretraining. “Video” labels means the method requires a video-level label of the action category in order to sample video pairs of the same category. “Phase” labels means the method uses annotations for the positions of the action phase boundaries in time, but not the action phase categories. “Frame” labels means the method uses fully labelled data with phase boundaries and phase category labels. Methods TCC* and LAV* denoted versions where a separate model is trained for each Penn Action category.

Methods using additional supervision still have an advantage in the Phase Progression and Frame Retrieval tasks. However, we note that our MV-Former with Kinetics-400 pretraining achieves state-of-the-art performance in Phase Classification, surpassing even the fully-supervised version of VSP (VSP-F). For FineGym99 and FineGym288 classification, MV-Former is only surpassed by VSP-F.

B. Additional Visualizations

We present additional visualizations of the attention maps of the Learned Spatial Token Pooling layers in Figure 4. We note that MV-Former is quite effective at identifying the primary actor in each scene across a wide range of person scales. In the bottom left example, it correctly attends to the tennis player even though they only occupy a few spatial tokens of the feature grid and they are standing against a complex background with many people in bleachers. When the person occupies a moderate to large portion of the image frame, LSTP tends to devote more attention to the position of the person’s limbs, which is an essential cue for human action phases. Finally, we note that category-specify objects are typically not given much attention, such as the baseball bat in the top left example, or the weights in the top right example. Although these objects are not included in entity 1, they are sometimes excluded by entity 2, which attends to the background. The weights in the top right example show a good example of this phenomenon.

Table 5. Comprehensive comparison of results on Penn Action and FineGym, including methods that use full or weak supervision. For Penn Action we also include methods using Kinetics-400 pretraining. While VSP-F still holds the highest score in many metrics, it is a fully supervised method, requiring complete frame-level annotations to train. However, in phase classification, MV-Former with Kinetics-400 pretraining surpasses VSP-F, and without pretraining it comes close to matching it. For Phase Progress, MV-Former is only surpassed by VSP-F. The Retrieval metric still strongly favors methods trained with additional supervision. For Kendall’s Tau, MV-Former has the highest average score, however the small changes in the Tau metric are not statistically significant. For both FineGym splits, MV-Former is second only to VSP-F. The highest score for each metric is **bold** and the second highest is underlined.

Method	Labels	Pretrain	Penn Action			FineGym	
			Classification	Progress	Tau	Retrieval	Class. (99)
TCC* [13]	Video	-	81.35	0.664	0.701	76.74	25.18
TCC [13]	Video	-	74.39	0.591	0.641	-	-
LAV* [20]	Video	-	84.25	0.661	0.805	79.13	-
LAV [20]	Video	-	78.68	0.625	0.684	-	-
GTA [19]	Video	-	-	0.789	0.748	-	-
SaL [29]	None	-	68.15	0.390	0.474	76.04	21.45
TCN [38]	None	-	68.09	0.383	0.542	77.84	20.02
CARL [8]	None	-	93.07	0.918	0.985	92.28	41.75
VSP [52]	None	-	93.12	0.923	0.986	92.56	43.12
VSP-P [52]	Phase	-	93.27	-	-	<u>93.45</u>	44.58
VSP-F [52]	Frame	-	<u>94.24</u>	-	-	94.89	45.66
CARL [8]	None	K-400	93.9	0.908	0.977	-	-
VSP [52]	None	K-400	93.57	0.944	<u>0.988</u>	-	-
MV-F (ours)	None	-	94.21 ± 0.04	<u>0.931 ± 0.006</u>	0.989 ± 0.002	92.99 ± 0.06	<u>44.77 ± 0.71</u>
MV-F (ours)	None	K-400	94.56 ± 0.32	0.924 ± 0.004	0.980 ± 0.002	93.40 ± 0.08	-

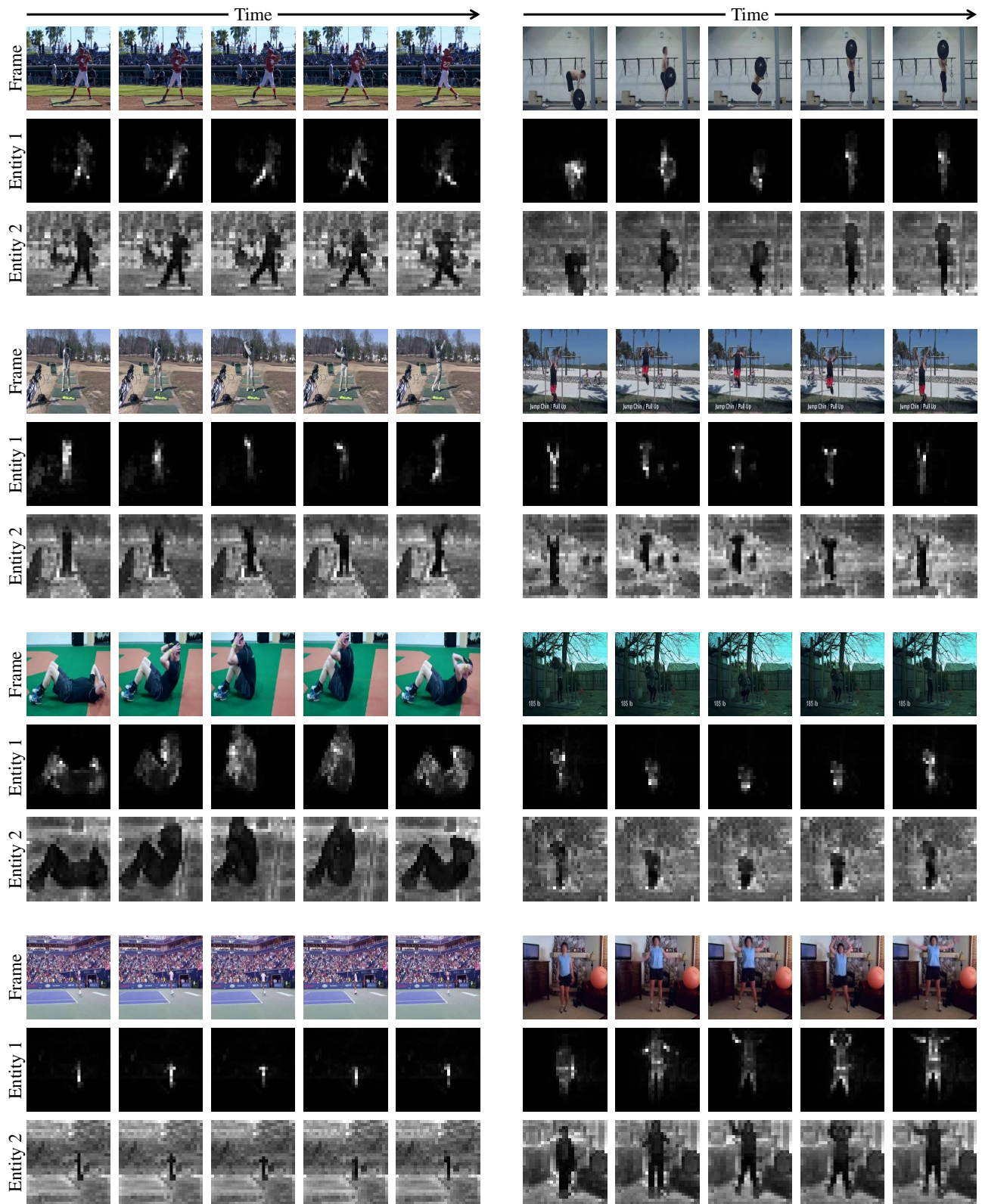


Figure 4. Additional visualizations of per-entity LSTP attention maps for sample videos from 8 categories of the Penn Action Dataset.